This is the peer reviewd version of the followng article:

Optimum Mechanical Design of Binary Actuators Based on Shape Memory Alloys / Spaggiari, A., Scire' Mammano, G., Dragoni, E. - In: Smart Actuation and Sensing Systems - Recent Advances and Future Challenges / Giovanni Berselli, Rocco Vertechy and Gabriele Vassura. - ELETTRONICO. - Rijeka : Intech, 2012. - ISBN 9789535107989. - pp. 1-32 [10.5772/50147]

Intech
Terms of use:

The terms and conditions for the reuse of this version of the manuscript are specified in the publishing policy. For all terms of use and more information see the publisher's website.

15/09/2026 20:42

(Article begins on next page)

Chapter 1

Optimum Mechanical Design of Binary Actuators Based on Shape Memory Alloys

A. Spaggiari, G. Scirè Mammano and E. Dragoni

Additional information is available at the end of the chapter

http://dx.doi.org/10.5772/50147

1. Introduction

Shape memory alloys are smart materials which have the ability to return to a memorized shape when heated. When an SMA is below its transformation temperature (martensitic phase), it has a low yield strength and can be deformed quite easily and behaves like a pseudoplastic solid. When the deformed material is heated above its transformation temperature there is a change in its crystal structure which causes the return to its original shape (austenitic phase). During this transformation the SMA element can generate a net force, behaving like an intrinsic actuator. The most common shape memory material is a nickel and titanium alloy called Nitinol [1]. SMAs have very good electrical and mechanical properties, high corrosion resistance and biocompatibility. When an electric current is injected in the SMA element, it can generate enough heat to cause the phase transformation due to joule effect. Thanks to their unique behaviour shape memory alloys have become a valuable industrial choice in the engineering world. Pseudo-plasticity, superelasticity, and shape memory effect [2] are increasingly used in many applications including actuators, constant-force springs, and adaptive damping systems. While the application of the superelastic effect is quite well established and understood for the manufacturing of medical devices with peculiar properties, the use of the shape memory effect for building solid state actuators is still characterized by a trial-and-error approach. Although the thermo mechanical phenomena behind the behaviour of SMAs are theoretically well known [3] - [4], there is an open challenge for engineering methods to assist the designer in exploiting these alloys for the development of industrial devices.

1.1. Design methodology review for SMA actuators

Many SMAs applications have been studied in recent years. Kuribayashi [5] proposes a rotary joint based on a bending SMA actuator, while, in [6] design and applications of SMA

INTECH
open science | open minds

© 2012 Spaggiari et al., licensee InTech. This is an open access chapter distributed under the terms of the Creative Commons Attribution License (http://creativecommons.org/licenses/by/3.0), which permits unrestricted use, distribution, and reproduction in any medium, provided the original work is properly cited.

actuators are presented. Microrobots can be developed using SMA as shown in [7] where there is a basic method to design the SMA spring based on a thermo-electromechanical approach. Reynaerts et al. [8] present design considerations concerning the choice of the active element to evaluate SMA actuator efficiency. Lu et al. [9] design a high strain shape memory actuator taking into account pseudoplasticity and compared its performance with traditional actuators. Due to SMA high non linearity, design curves relying on experiments are proposed in [10] to assess the SMA actuator geometry. A comprehensive review of applications of SMAs in the field of mechanical actuation has recently been published in [11]. Jansen et al [12] develop a linear actuator used as a drive module in an angular positioning mini-actuator. This architecture allows both large force and long strokes to be obtained. Strittmatter et al. [13] propose a SMA actuator for the activation of a hydraulic valve, biased by a conventional spring. Bellini et al. [14] propose a linear SMA actuator able to vary the air inflow for internal combustion engines, improving gas combustion and leading to higher efficiency. Haga et al. [15] propos a mini-actuator to be used in Braille displays. Elwaleed et al. [16] develop a SMA beam actuator able to amplify the SMA actuator strain using elastically instable beams. Among the proposed actuator there is lack of simple design instruments to provide basic information to the designer, either due to specific constraints of application or due to the high complexity of the thermomechanical material models used. In order to answer for an analytical design methodology, the author described in several technical publications a set of equations useful for linear [18] and rotary application [19]. The authors developed the design equations both for SMA actuators under a general system of external forces [20] and produced the design formulae to increase the output stroke thanks to negative stiffness compensators [21]. Moreover two peculiar systems were designed and developed: a telescopic actuator [22] and a wire on drum system [23]. The present work reviews and improves the design rules developed by the authors and set them in a coherent formal analytical framework. Design examples are provided to illustrate the step-by-step application of the design optimization procedures for realistic case studies.

1.2. Challenges and issues in SMA actuators design

The three main challenges in SMA actuator design are: obtaining a simple and reliable material model, increasing the stroke of the actuator and finding design equations to guide the engineer in dimensioning the actuator. To design SMA actuators, a material model must describe the mechanical behaviour of the alloy in two temperature ranges: below the temperature M_f, at which the austenite-martensite transformation is finished (OFF or deactivated or cold state) and above the temperature, A_f, at which the martensite-austenite transformation is completed (ON or activated or hot state). In these two conditions, inside the shape memory material there is only one stable crystalline phase and therefore the macroscopic mechanical properties are known.

The authors proposed two simple material models to describe SMA behaviour, both of them describing the mechanical behaviour of a SMA element at high temperatures (austenitic phase) as linear, characterized by the elastic modulus E_A. The first one approximates the martensitic

behaviour as a linear one [18] (Figure 1a). This behaviour is by no means obvious, thus an explanation is needed. The typical stress-strain curve of a shape memory material, shown in Figure 1a, has two characteristic paths corresponding to a low temperature (martensitic curve) and to a high temperature (austenitic curve). Both curves consist of an initial elastic portion (OA and OC), followed by a constant-stress plateau. In the practical use of shape memory alloys for making actuators, the materials remain within the linear elastic range at the higher temperature but are strained beyond the elastic limit when cooled to the lower temperature. The maximum strain, ε_{adm} is small enough to ensure the desired fatigue life [24-25] but large enough to maximize the stroke of the actuator for a given amount of material involved. Since this analysis is aimed at dimensioning the binary actuator for the extreme positions, irrespective of the intermediate state, the behaviour of the material is approximated by segments OA' (martensite) and OC (austenite) in Figure 1a. The reference elastic moduli are E_M and E_A, respectively. This is also true if the shear behaviour of the shape memory material is considered, when the maximum shear strain, γ_{adm}, replaces ε_{adm} and the shear moduli G_M and G_A replace E_M and E_A.

The second material model describes the behaviour at cold temperatures (martensitic phase) with a bilinear law [21] as shown in the stress-strain diagram of Figure 1b. The model is defined by a first leg OD with an elastic modulus E_{MA} and a second leg DE with a gradient E_{MB}. We define ε_g as the deformation of the occurrence of the change of slope. Due to the bilinear stress-strain response, the SMA elements used in the actuators (springs or wires) also have bilinear force-displacement behaviour when disabled. The elastic moduli E_A, E_{MA} and E_{MB} are replaced by the stiffness K_A, K_{MA}, K_{MB}, while the deformation ε_g is replaced by the displacement x_g. Assuming that the geometric changes related to the deformations of the springs do not influence the elastic constant value, a parameter of merit of the SMA material, s_1, can be defined as follows:

$$s_1 = \frac{E_A}{E_M} = \frac{G_A}{G_M} = \frac{k_a}{k_m} \tag{1}$$

This non dimensional group expresses for both models the shape memory capability of the alloy, the larger s_1 the better the material is. The only difference is that in case of the simplest linear model (Figure 1a) the denominator is the secant modulus, while in case of bilinear model (Figure 1b) the denominator is E_{MA} the modulus of the first linear martensitic region. In order to balance the active SMA element authors evaluates the influence of three backup elements: a constant force (Section 3.1) a conventional spring (Section 3.2) and an antagonistic SMA (Section 3.3). Moreover the authors propose two compensator systems in order to increase the stroke of the actuator. The systems are either based on a leverage (rocker-arm, Section 4.2.1) or on articulated mechanisms (double quadrilateral, Section 4.2.2), which can be considered as backup elements with negative stiffness.

2. Design procedure of binary SMA actuators

In this section a design procedure for binary SMA actuators is described and discussed. The system is made up by a generic actuator which moves the output port by means of an elastic system containing an active SMA element and a bias (backup) element.

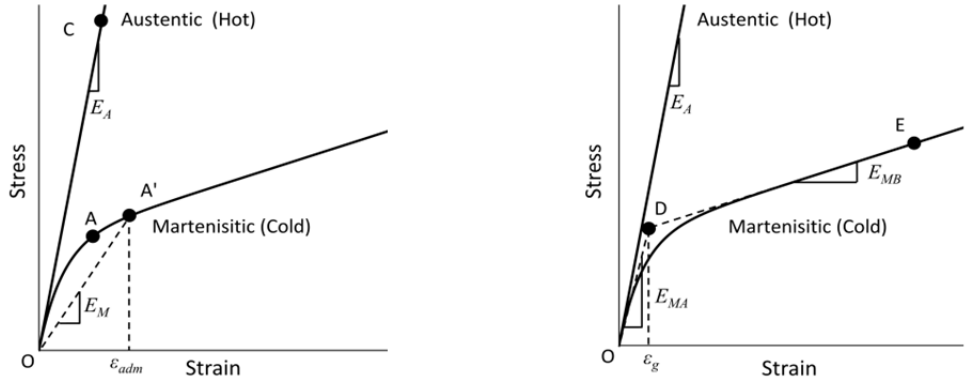

Figure 1. Linear (a) and bilinear (b) material model for martensitic phase of SMA elements

According to the particular means of applying the bias force, the three cases shown in Figure 2 are analyzed:

- a primary SMA spring biased by a constant force (Figure 2a);
- a primary SMA spring biased by a traditional spring (Figure 2b);
- two antagonist SMA springs (when one is hot, the other one is cold, Figure 2c).

Without loss of generality, each spring in Figure 2 is modeled as a traction spring exhibiting a linear force-deflection relationship. While the assumption of linearity is obvious for the traditional spring in Figure 2b, the linear behaviour for the SMA spring is an approximation needed to use the model in Figure 1a.

Each actuator presented in Figure 2 is intended to move the output port E through a total useful stroke Δx when working against an external dissipative force F_F and an external conservative force F_0. The force F_F is always opposite to the velocity of the cursor and is assumed to be constant. For example, if the cursor is subject to dry friction forces characterized by a static value F_S and a dynamic value $F_D < F_S$, the design dissipative force $F_F = \text{MAX}(F_S, F_D) = F_S$ will be adopted for the calculation.

This approach comprises every possible external constant load, as exemplified by the membrane pump shown in Figure 3a. This example represents the most general case of external constant forces the actuator has to deal with. The SMA actuator undergoes the following external loads: two generic dissipative forces F_1 (force during aspiration) and F_2 (force during pumping) and a conservative force F_u due to the gravity force on the piston. The dissipative force F_1 and the force F_u act together against the primary spring, when the piston is moving towards the primary SMA spring (inlet of the fluid). By contrast, the dissipative force F_2 acts on the cursors against the force F_u and the primary spring, when the cursor moves away from the primary SMA spring (outlet of the fluid). This force system can

be always reduced to the two forces considered in the method: a conservative one, F_0 and two symmetric dissipative ones, F_F, rearranging the forces as follows:

$$F_0 = F_u + \frac{F_1 - F_2}{2} \quad , \quad F_F = \frac{F_1 + F_2}{2} \tag{2}$$

The direction of the forces depends on the piston speed, v, as shown in Figure 3b-c.

A second non dimensional parameter, s_2, useful in the configurations with two springs, is defined as the ratio between the minimum value assumed by the stiffness of bias spring 2 and the stiffness of active spring 1 in the cold state:

$$s_2 = \frac{K_{2\min}}{K_{1SC}} \tag{3}$$

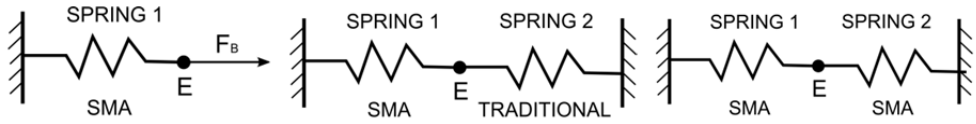

(a) (b) (c)

Figure 2. Three cases of the shape memory actuator biased by: a constant force (a), a traditional spring (b), a shape memory spring (c).

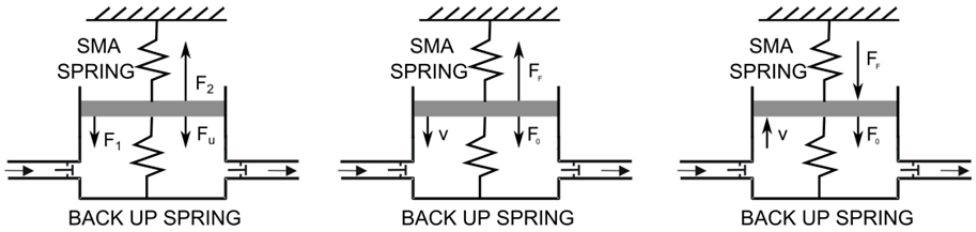

(a) (b) (c)

Figure 3. Example of generic conservative and dissipative forces acting on the system (a), equivalent forces when SMA is inactive (b) and when SMA is active (c)

The minimum value assumed by the stiffness of spring 2, K_{2min}, coincides with the only stiffness of spring 2, K_{2C}, if spring 2 is a traditional one, while it coincides with K_{2SC} if spring 2 is an active one. A third dimensionless parameter, s_F, is introduced in order to consider the influence of the dissipative forces in the motion of the SMA actuator. This parameter is defined as the ratio between the dissipative force F_F and the maximum force sustained by the primary spring in the cold state, calculated as the product between the cold spring stiffness, K_{1SC}, and the maximum deflection, L_C-L_{01}, in the cold state:

$$s_F = \frac{F_F}{K_{1SC} \cdot \left(L_C - L_{01}\right)} \tag{4}$$

The fourth dimensionless parameter, s_0, is introduced in order to consider the influence of the conservative force in the motion of the SMA actuator. This parameter is defined as the ratio between the conservative force F_0 and the maximum force sustained by the primary spring in the cold state, calculated as the product between the cold spring stiffness, K_{1SC}, and the maximum deflection, L_C-L_{01}, in the cold state:

$$s_0 = \frac{F_0}{K_{1SC} \cdot \left(L_C - L_{01}\right)} \tag{5}$$

The combination of definitions (4) and (5) gives the relationship between s_F and s_0:

$$s_0 = \frac{F_0}{F_F} \cdot s_F \tag{6}$$

2.1. SMA actuator backed up by a constant force

Figure 4a shows the actuator biased by a constant force in three characteristic positions. Figure 4b shows the relationship between the applied force and the spring deflection during the travel of the actuator between these positions.

The procedure can be retrieved from [20]. The useful stroke of the actuator is obtained as:

$$\Delta x = \frac{F_B}{K_{1SC}} \cdot \frac{\left(s_1 - 1 - 2s_F\right)}{s_1 \cdot \left(s_F + 1 - s_0\right)} \tag{7}$$

The bias force is:

$$F_B = F_F \cdot \frac{s_F + 1 - s_0}{s_F} \tag{8}$$

Thus, the stroke can be cast as:

$$\Delta x = \left(L_C - L_{01}\right) \frac{s_1 - 1 - 2s_F}{s_1} \tag{9}$$

Eq. (7) shows that meaningful strokes ($\Delta x > 0$) are only possible if parameter s_F is lower than the following critical value.

$$s_{Fcr} = \frac{s_1 - 1}{2} \tag{10}$$

Moreover, a possible way to choose the value of s_F consists on studying the free length of the active spring, L_{01}, and its wire diameter, d_1, as described below in eq. 14.

2.1.1. Embodiment of SMA actuator

If helical springs or wires are considered, two fundamental expressions can be written for the diameter or the wire and for the length of the springs, as a function of the stiffness, K and of the deflection of the SMA element, f.

$$d = m_d \cdot \sqrt{K \cdot f} \tag{11}$$

$$L_0 = m_l \cdot f \tag{12}$$

The constant m_d and m_f depends on the embodiment and can be calculated as shown in the examples in Section 3.1.2 and Section 3.2.2.

A generic expression of the free length, L_{01}, can be written as follows:

$$L_{01} = m_l \cdot \Delta x \cdot \frac{s_1}{s_1 - 2 \cdot s_F - 1} \tag{13}$$

In (13) the free length, L_{01}, depends on the particular embodiment of the spring, but it is always minimized if s_F is chosen as small as possible. The minimum value of s_F can be determined by fixing the maximum allowable wire diameter, d_1, of the SMA element. This maximum value can be determined, for example, using cooling time considerations, the bigger the wire, the slower the cooling, [8], [18].

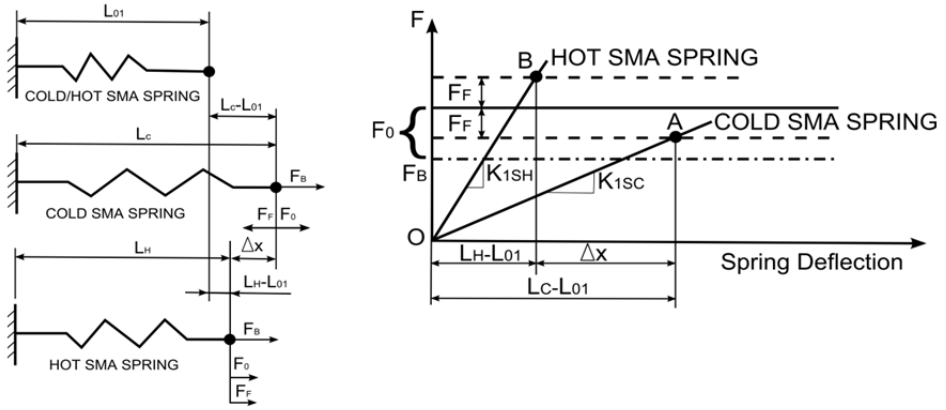

(a) (b)

Figure 4. Actuator model (a) and force-deflection diagram (b) of the shape memory actuator biased by a constant force

Combining expression (11) with (1) and (3), the following relationship can be used to determine the minimum value of s_F.

$$d_1 = m_{d1} \cdot \sqrt{\frac{F_F}{s_F}} \tag{14}$$

Where m_{d1} depends only on the embodiment of the SMA primary spring.

2.1.2. Case study: SMA wire based actuator

The equations (11) and (12) represent the relationships between stiffness, K, and free length, L_0, either for a spring or a wire.

In particular the stiffness of a SMA actuator in wire form is obtained using the coefficient:

$$m_{dw} = \sqrt{\frac{4}{\pi \cdot E_m \cdot \varepsilon_{adm}}} \tag{15}$$

where it is shown that the limit is given by the maximum strain of the SMA wire in martensitic phase. The free length is obtained from eq. (11) by considering the following coefficient for a SMA wire, which comes out simply from the definition of axial strain in a rod.

$$m_{lw} = 1 \Big/ \varepsilon_{adm} \tag{16}$$

2.2. SMA actuator backed up by an elastic spring

Figure 5a shows the actuator biased by a traditional spring in three characteristic positions. Figure 5b displays the relationship between the applied force and the deflection of each spring during the thermal operation of the actuator between those positions.

The detailed procedure can be retrieved from [20]. The pre-stretch is

$$p = \left(L_C - L_{01}\right) \frac{s_2 + s_F + 1 - s_0}{s_2} \tag{17}$$

$$\Delta x = p \frac{s_2 \cdot \left(s_1 - 2 \cdot s_F - 1\right)}{\left(s_1 + s_2\right) \cdot \left(s_2 + s_F + 1 - s_0\right)} \tag{18}$$

The following alternative expression of the overall travel can be written

$$\Delta x = \left(L_C - L_{01}\right) \frac{s_1 - 1 - 2s_F}{s_1 + s_2} \tag{19}$$

Lastly, Figure 5b shows that the maximum deflection in the cold state of the bias spring amounts to $p-(L_H-L_{01})$. This expression can be written as:

$$p-\left(L_H-L_{01}\right)=\left(L_C-L_{01}\right)\cdot\frac{s_1\cdot\left(s_2+s_F+1\right)-s_2\cdot s_F-s_0\cdot\left(s_1+s_2\right)}{s_2\cdot\left(s_1+s_2\right)} \tag{20}$$

2.2.1. Embodiment of the SMA actuator

If helical springs or wires are considered, the two fundamental expressions (11) and (12) can be written for the diameter of the wire and for the length of each spring. Following [20] a generic expression of the total length can be obtained, which depends on the dimensionless parameters s_1, s_2, s_0 and s_F and on the embodiment of the springs.

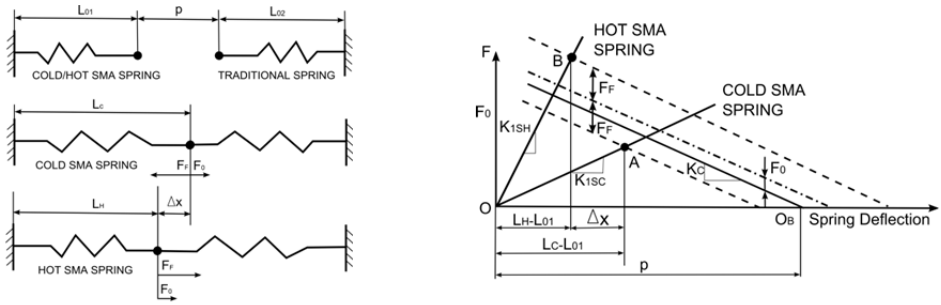

Figure 5. Actuator model (a) and force-deflection diagram (b) of the shape memory actuator biased by a traditional spring

This expression is minimized if s_F is chosen as small as possible and if a precise value of s_2^* is chosen, obtained by equating to zero the derivative of the total length of the actuator. The optimal value s_2^* can be expressed as:

$$s_2^*=\sqrt{\frac{s_1\cdot\left(m_{l2}+1\right)\cdot\left(s_F+1-s_0\right)}{\left(m_{l1}+1\right)}} \tag{21}$$

As a first attempt, it is possible to determine the m_l coefficients considering the desired embodiment of each spring and a value of C = 7, because the value of s_2^* is not greatly affected by C.

2.2.2. Case study: SMA spring based actuator

The equations (11) and (12) represent the relationships between stiffness, K, and free length, L_0, either for a spring or a wire.

In particular the wire diameter of a helical spring can be cast as follows [26]:

$$d=\sqrt{\frac{4\cdot K\cdot f\cdot K_b}{\pi\cdot G\cdot\gamma_{adm}}} \tag{22}$$

Were K is the stiffness of the spring, f is the deflection of the spring and K_b is the coefficient of Bergstrasser, given by the following relationship:

$$K_b = \frac{4 \cdot C + 2}{4 \cdot C - 3} \tag{23}$$

Thus for a spring the m_{ds} coefficient in expression (11) can be expressed as:

$$m_{ds} = 4\sqrt{\frac{(C+2)}{\pi \cdot G \cdot \gamma_{adm} \cdot (4C-3)}} \tag{24}$$

The external diameter of a helical spring can be calculated using the definition of the spring index ($C = D/d$) and the number of active coils is given by:

$$N = \frac{G \cdot d}{8 \cdot C^3 \cdot K} \tag{25}$$

The fully compressed length can be calculated using expression:

$$L_{fc} = Nd = \frac{G \cdot d^2}{8 \cdot C^3 \cdot K} \tag{26}$$

The free length is:

$$L_0 = 1.15 \cdot Nd + f = 1.15 \cdot \frac{G \cdot f \cdot d^2}{8 \cdot C^3 \cdot F} + f \tag{27}$$

Thus the coefficient to calculate the free length in eq. (12) is:

$$m_{ls} = \frac{1.15 + \pi \cdot \gamma_{adm} \cdot C^2}{\pi \cdot \gamma_{adm} \cdot C^2} \tag{28}$$

2.3. SMA actuator backed up by an antagonist SMA spring

Figure 6a shows the actuator biased by a second SMA spring in three characteristic positions. Figure 6b shows the relationship between the applied force and the deflection of each spring during the thermal operation of the actuator between these positions.

Following the procedure described in [20], the prestretch p can be written:

$$p = (L_C - L_{01}) \cdot \frac{s_1 \cdot s_2 + s_F + 1 - s_0}{s_1 \cdot s_2} \tag{29}$$

The stroke can be cast as:

$$\Delta x = p \cdot \frac{s_2 \cdot \{(s_1 - 1 - s_F) \cdot (s_1 + 1) - s_0 \cdot (s_1 - 1)\}}{(s_1 + s_2) \cdot (s_1 \cdot s_2 + s_F + 1 - s_0)} \tag{30}$$

The following expression for the optimal value s_2^* is found:

$$s_2^* = \sqrt{s_F + 1 - s_0} \tag{31}$$

The following alternative expression of the overall travel can be obtained:

$$\Delta x = \left(L_C - L_{01}\right) \cdot \frac{\left(s_1 - 1 - s_F\right) \cdot \left(s_1 + 1\right) + s_0 \cdot \left(s_1 - 1\right)}{s_1 \cdot \left(s_1 + s_2\right)} \tag{32}$$

Both Equations (30) and (32) demonstrate that meaningful strokes ($\Delta x > 0$) are only possible if parameter s_F is lower than the following critical value.

$$s_{Fcr} = \frac{F_F \cdot \left(s_1 - 1\right)^2}{F_0 \cdot \left(s_1 - 1\right) + F_F \cdot \left(s_1 + 1\right)} \tag{33}$$

Figure 6b shows that the maximum deflection of the bias spring in the cold state amounts to $p - \left(L_H - L_{01}\right)$. This expression can be written as:

$$p - \left(L_H - L_{01}\right) = \left(L_C - L_{01}\right) \cdot \frac{s_1 \cdot s_2 - s_2 \cdot s_F + s_F + 1 - s_0 \cdot \left(s_2 + 1\right)}{s_2 \cdot \left(s_1 + s_2\right)} \tag{34}$$

2.3.1. Embodiment of SMA antagonist actuator

If helical springs or wires are considered, the two fundamental expressions (11) and (12) can be written for the diameter of the wire and for the length of each spring. Following [20] a generic expression of the total length can be obtained, which depends on the dimensionless parameters s_1, s_2, s_0 and s_F and on the embodiment of the springs.

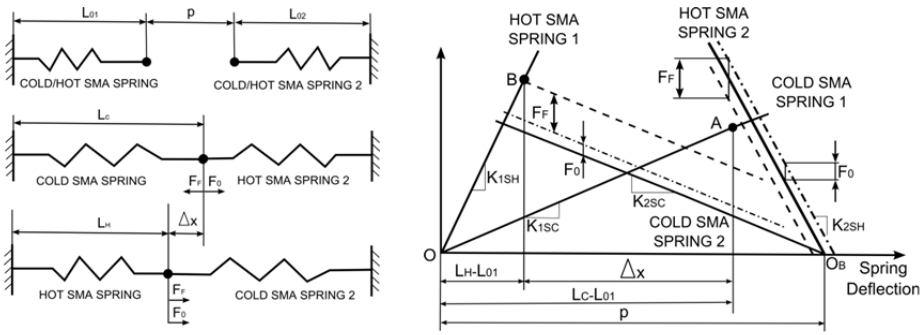

Figure 6. Actuator model (a) and force-deflection diagram (b) of the agonist antagonist shape memory actuator

This expression is minimized if s_F is chosen as small as possible and if an optimal value for s_2^* is chosen, obtained equating to zero the derivative of the total length of the actuator. The optimal value s_2^* can be expressed as:

$$s_2^* = \sqrt{\frac{(m_{l2}-1)\cdot(s_F+1-s_0)}{(m_{l1}-1)}} \tag{35}$$

Expression (35) reduces to expression (31) if the same spring embodiment is considered for spring 1 and spring 2. As a first attempt, it is possible to determine the m_l coefficients considering the desired embodiment of each spring and a value of C = 7, because the value of s_2^* is not greatly affected by C. The minimum value of s_F can be determined by fixing the maximum allowable wire diameter, d_l, of the SMA element. This maximum value can be determined, for example, using cooling time considerations. Relationship (14) can be used to determine the minimum value of s_F.

2.4. Design procedures for a binary SMA actuator

The step by step procedures which guide the designer to apply the above design methods are described in Table 1. The first four steps are the same irrespective of the backup element used in the actuator. From step 5, the procedure is threefold.

These procedures ensure that any actuator biased by a one of the above described back up elements, with the calculated stiffness K_C and containing whatever SMA spring, with the selected material parameter s_1 and the calculated cold stiffness K_{ISC}, satisfies the design problem (useful stroke Δx, design dissipative force F_F and design conservative force F_0) when assembled with the calculated pre-stretch p.

2.4.1. Case study: SMA based swing louver

In this section, the complete design procedure is carried out numerically for the actuation of a swing louver exploited to direct the air flow in domestic air conditioners. An actuator made up of an SMA spring biased by an antagonist SMA spring is designed here as a possible alternative solution to conventional electric motors and linkages. The SMA actuator acts on the louver with a known arm to make the louver swing. The design parameters are: required stroke: 5mm; dissipative force: 5N, conservative force: 2N. The material considered is Nitinol, with the following properties, γ_{adm} = 0.02, to ensure a fatigue limit over 500 thousand cycles, austenitic shear modulus G_a=23000 MPa, equivalent martensitic shear modulus G_m=8000 MPa.

The procedure starts calculating the non dimensional groups from eq. (1), (10), (31) and (5):

$$s_1 = \frac{G_A}{G_M} = \frac{23000}{8000} = 2.875 \tag{36}$$

Backup: Constant Force (Section 3.1)	**Backup: Traditional spring (Section 3.2)**	**Backup: antagonist SMA spring (Section 3.3)**
—the stroke of the actuator, Δx, the design dissipative force, F_F, and the design conservative force, F_0, are accepted from design specifications; —a shape memory material for the spring and a maximum strain, ε_{adm} or γ_{adm}, are selected, after which parameter $s_1 = E_A/E_M = G_A/G_M$ is known; —The spring embodiment is chosen and the parameters ml_1, ml_2 and md_1 are calculated as shown in Section 3.1.2 or 3.2.2. Otherwise, this step is skipped; —a s_F value lower than the critical value (10) is selected, possibly using (14);		
—the value of s_0 is calculated using definition (6); —the bias force, F_B, is calculated using eq. (8); —the maximum deflection of the primary spring, L_C-L_{01}, is retrieved from (9); —the cold stiffness, K_{1SC}, of the spring is calculated from eq. (7);	—the value of s_0 is calculated using definition (6); —the lowest affordable value of parameter s_2 is chosen (to exploit the primary spring), or the optimal value (21) is adopted (to conserve overall space). If the parameters ml_1 and ml_2 cannot be determined, expression (31) can be used for a sub-optimal design; —the maximum deflection of the primary spring, L_C-L_{01}, is retrieved from (19); —the cold stiffness, K_{1SC}, of the spring is calculated from eq. (4); —the pre-stretch of the system, p, is calculated from (17); —the stiffness of the traditional spring, K_C, is calculated from eq. (3); —the maximum deflection of the traditional spring, p-$(L_H$- $L_{01})$, is calculated from (20).	—a s_F value lower than the critical value (10) is selected. The parameter is chosen as small as possible to reduce the size of the actuator, respecting the constraint of the diameter of the wire, d, given by (14); —the value of s_0 is calculated using definition (6); —the lowest affordable value of parameter s_2 is chosen (to exploit the primary spring), alternatively the optimal value (35) is adopted (to conserve overall space). If the parameters ml_1 and ml_2 cannot be determined, expression (31) can be used for a sub-optimal design; —the maximum deflection of the primary spring, L_C-L_{01}, is retrieved from (32); —the cold stiffness, K_{1SC}, is calculated from eq. (4); —the overall pre-stretch of, p, is calculated from (29); —the stiffness of the secondary SMA spring, K_{2SC}, is calculated from eq. (3); —the maximum deflection of the secondary SMA spring, p-$(L_H$- $L_{01})$, is calculated from (34).

Table 1. Step by step procedure for each Backup element considered

$$s_{Fcr} = \frac{s_1 - 1}{2} = \frac{2.875 - 1}{2} = 0.9375 \tag{37}$$

$$s_F = 0.25 \le s_{Fcr} \tag{38}$$

$$s_2 = s_2^* = \sqrt{s_1 \cdot (s_F + 1)} = \sqrt{2.875 \cdot (0.25 + 1)} = 1.896 \tag{39}$$

$$s_0 = \frac{F_0}{F_F} \cdot s_F = \frac{2}{5} \cdot 0.25 = 0.1 \;\; s_0 = \frac{F_0}{F_F} \cdot s_F = \frac{2}{5} \cdot 0.25 = 0.1 \tag{40}$$

the maximum deflection of the primary spring, L_C-L_{01}, is retrieved from (32);

$$\begin{aligned} (L_C - L_{01}) &= \Delta x \cdot \frac{s_1 \cdot (s_1 + s_2)}{(s_1 - 1 - s_F) \cdot (s_1 + 1) + s_0 \cdot (s_1 - 1)} = \\ &= 5 \cdot \frac{2.875 \cdot (2.875 + 1.896)}{(2.875 - 1 - 0.5) \cdot (2.875 + 1) + 0.1 \cdot (2.875 - 1)} = 12.43\,mm \end{aligned} \tag{41}$$

while eq. (4) allows the SMA spring cold stiffness to be calculated

$$K_{1SC} = \frac{F_F}{s_F \cdot (L_C - L_{01})} = \frac{5}{0.25 \cdot 12.43} = 1.61\,N/mm \tag{42}$$

the overall pre-stretch of, p, is calculated from (29) and K_C, is calculated from eq. (3)

$$p = (L_C - L_{01}) \cdot \frac{s_1 \cdot s_2 + s_F + 1 - s_0}{s_1 \cdot s_2} = 12.43 \cdot \frac{2.875 \cdot 1.896 + 0.25 + 1 - 0.1}{2.875 \cdot 1.896} = 15.01\,mm \tag{43}$$

$$K_{2\min} = K_{2SC} = s_2 \cdot K_{1SC} = 1.896 \cdot 1.61 = 3.052\,N/mm \tag{44}$$

$$\begin{aligned} p - (L_H - L_{01}) &= (L_C - L_{01}) \cdot \frac{s_1 \cdot s_2 - s_2 \cdot s_F + s_F + 1 - s_0 \cdot (s_2 + 1)}{s_2 \cdot (s_1 + s_2)} = \\ &= 12.43 \cdot \frac{2.875 \cdot 1.896 - 1.896 \cdot 0.25 + 0.25 + 1 - 0.1 \cdot (1.896 + 1)}{1.896 \cdot (2.875 + 1.896)} = 8.16\,mm \end{aligned} \tag{45}$$

the maximum deflection of the secondary SMA spring, p-(L_H-L_{01}), is calculated from eq. (34).

The detailed design of primary SMA spring is given by combination of eq. (11) and (24) regarding the spring wire diameter, considering a spring index $C=7$

$$d = 4\sqrt{\frac{(C+2) K_{1SC} (L_C - L_{01})}{\pi \cdot G \cdot \gamma_{adm} \cdot (4C - 3)}} = 4\sqrt{\frac{(7+2) \cdot 1.61 \cdot 12.43}{\pi \cdot 8000 \cdot 0.02 \cdot (4 \cdot 7 - 3)}} = 0.48\,mm \tag{46}$$

the free length of the primary spring is given by the combination of eq. (12) and (28)

$$L_0 = \frac{1.15 + \pi \cdot \gamma_{adm} \cdot C^2}{\pi \cdot \gamma_{adm.} C^2} \cdot \left(L_C - L_{01} \right) = \frac{1.15 + \pi \cdot 0.02 \cdot 7^2}{\pi \cdot 0.02 \cdot 7^2} \cdot 12.43 = 17.07\, mm \tag{47}$$

The same procedure is applied to calculate the design parameter of the antagonist spring.

3. Design of compensated SMA actuators

SMA based actuators develop significant forces but are usually characterized by low strokes. The stroke is primarily limited by the maximum strain that the alloy can withstand for the expected life as shown in [24], [25]. The backup element needed to recover the stroke prevents the SMA element from recovering completely its shape is a further cause of stroke loss. Furthermore, the force delivered by shape memory actuators varies linearly with the displacement while the external load is usually constant. The design of a SMA actuator ensures that the minimum actuator force is sufficient to contrast the external load [18], providing an additional cause of stroke reduction.

This section introduces a compensation system to store available power from the SMA element in high force positions and then return this power in low force positions [19]. The same principle was successfully applied for electroactive polymer actuators by introducing compliant mechanisms [27]. The compensation system adopted has a negative elastic characteristic, generating a decreasing force as the deformation increases.

3.1. Principle of elastic compensation

The force-deflection diagram in Figure 7 shows the characteristic lines of an SMA actuator in the austenitic (hot SMA, solid circles) and martensitic (cold SMA, solid squares) states. When the SMA element is backed up by a linear spring with the linear characteristic shown with hollow triangles, the net stroke under no external force is S_{spring}. Starting from the same maximum deflection and force of the cold SMA, the stroke increases to S_{weight} when the active element is backed up by a constant force (crossed horizontal line). The improvement is consequent upon the reduced stiffness (lower contrasting forces) of the backup element which allows the SMA to recover a greater share of deformation.

By learning from this positive trend, it is easily seen that an even greater stroke (S_{comp}) is achieved if the backup element displays a negative slope (hollow circles) so that the contrast force would decrease with increasing deflection. Energetically, the compensation system accumulates energy from the SMA element in the positions where the SMA force is high (right-hand side in Figure 7) and releases that energy to the actuators in the positions where the SMA force is low (left-hand side in Figure 7).

As shown in the subsequent sections, a backup element with negative slope as in Figure 7 can be achieved by exploiting one of the many spring-assisted mono or bistable mechanisms described in the technical literature. The use of an elastic compensation system requires the introduction of hard stops to prevent the SMA elements from over-straining. In the case of a single-SMA actuator (see Figure 7), a single hard stop is needed and the behaviour in the

absence of power becomes monostable. In the case of a double-SMA actuator, two hard stops are required and the behaviour in the absence of power becomes bistable. Although the advantages of the compensation system in terms of force and stroke apply to both single-SMA and two-SMA actuators, the improvements are more pronounced for the two-SMA actuator. The general theory [21] demonstrates that a single-SMA actuator can generate a truly constant output force on only one direction of motion. By contrast, a two-SMA actuator can achieve a constant-force profile in both directions. Further advantages of the compensated architecture over regular SMA actuators are the existence of definite equilibrium positions when the power is shut off, the enforcement of precise mono (single-SMA) or binary (two-SMA) positioning, and the possibility of easy control strategies. The input data required for the design of a shape memory actuator are the value of the guaranteed minimum useful force in the two directions of activation (F_{ON}, F_{OFF} in the case of a single SMA element, F_{ON1}, F_{ON2} when there are two opposing SMA elements), the value of the stroke desired, S, and the type of alloy used for the active elements (i.e. s_1, s_m, s_g).

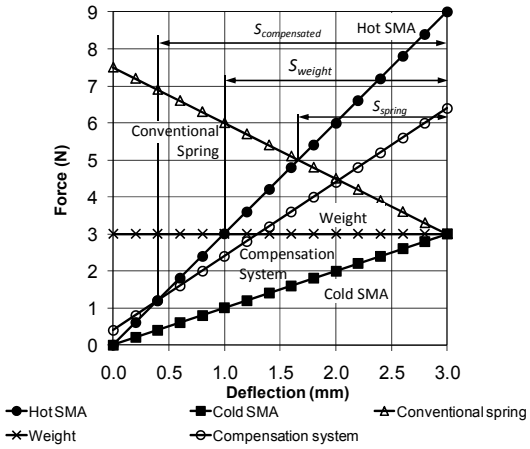

Figure 7. Force-deflection curves of a single-SMA actuator backed up by: a conventional spring, a constant force and an elastic compensation system

3.2. Material model: Definitions

In order to design compensated shape memory actuators the bilinear model for the martensitic state of SMA (Figure 1b) was used. Since ε_g (then x_g) is very small ($0.2\% < \varepsilon_g < 0.5\%$) the force-stroke characteristic of the SMA elements can be approximated as a linear trend (D'E in Figure 8), with slope K_{MB}, starting from the force F_{0m} in correspondence to zero displacement (Figure 8). The force F_{0m} is calculated as:

$$F_{0m} = \left(K_{MA} - K_{MB}\right) x_g \tag{48}$$

The force F_{SMA_ON} produced by the generic shape memory element in the activated state (austenite) is given by the line OC in Figure 8 and is:

$$F_{SMA_ON} = K_A x \tag{49}$$

In the cold state (martensite), the force F_{SMA_OFF} is given by the line D'E in Figure 8:

$$F_{SMA_OFF} = F_{0m} + K_{MB} x \tag{50}$$

In addition to s_1 already defined in eq. (1), to facilitate the design of the actuator, it is useful to define two other dimensionless coefficients:

$$s_m = \frac{E_{MB}}{E_{MA}} = \frac{K_{MB}}{K_{MA}} \tag{51}$$

$$s_g = \frac{\varepsilon_g}{\varepsilon_{adm}} = \frac{x_g}{x_{adm}} \tag{52}$$

The parameter s_m is the ratio between the two stiffness of the alloy at cold temperatures and it is a characteristic of the shape memory material. The parameter s_g is the ratio of the deflection, x_g, at which the change in stiffness in the martensitic state is recorded and the maximum allowable deflection x_{adm}, related to the maximum deformation, ε_{adm}, admissible for the material. To limit the size of the device, it is convenient to assume the $x_{maz} = x_{adm}$ so as to completely exploit the material.

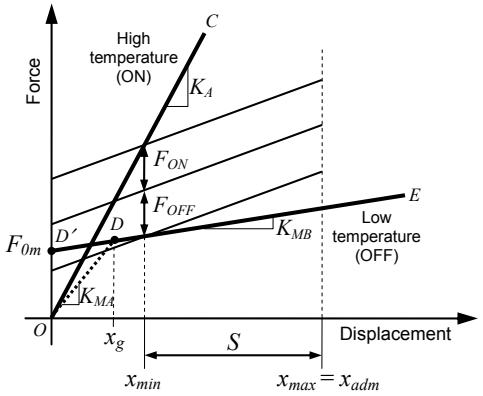

Figure 8. Force-deflection curves of a two-SMA actuator superimposed on the characteristic lines of the compensator.

3.3. Design of compensated single SMA actuators

To design compensated actuators with a single SMA element, it is convenient to introduce the ratio, γ, between the stroke and the maximum deflection of the SMA element:

$$\gamma = S / x_{adm} \tag{53}$$

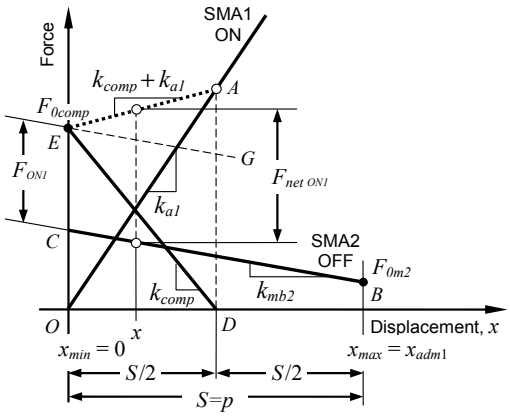

Figure 9. Force-deflection curves of a two-SMA actuator compensated by a generic negative elastic spring (line *ED*)

The axial dimension of the actuator is reduced as the ratio γ tends to one because in this case all the deformation that the material can sustain is used to produce a useful stroke. However, the value γcannot reach the unity because the minimum deflection would be zero and the SMA element would not be able to exert any useful force.

The force delivered by the shape memory element can be calculated with (49), in the austenitic state, and with the approximated expression (50), in the martensitic state. Figure 8 shows that the high-temperature curve (OC) and the low-temperature curve (A'B) diverge. Thus, the most unfavorable position in which the design force is required is where the difference between the two curves (useful force) is minimal. In this position, the sum of the design forces in both directions must equal the distance between the ON straight line and the OFF straight line. Assuming conventionally $F_{ON} > 0$ (because it agrees with the force exerted by the SMA element) and $F_{OFF} < 0$ (because it is opposed to the force produced by the SMA) we have $(F_{ON} - F_{OFF}) = F_{SMA_ON}\ (x = x_{min}) - F_{SMA_OFF}\ (x = x_{min})$. Recalling (48),(49),(50) and introducing the dimensionless parameters (1),(51),(52) this condition becomes:

$$F_{ON} - F_{OFF} = \frac{k_{MA} S}{\gamma}\left[\left(s_1 - s_m\right)\left(1-\gamma\right) - s_g\left(1 - s_m\right)\right] \tag{54}$$

The stiffness needed to fulfill the minimum force in both directions and to achieve the desired stroke is obtained by solving (54) with respect to the stiffness k_{MA}:

$$k_{MA} = \frac{\gamma\left(F_{ON} - F_{OFF}\right)}{S\left[\left(s_1 - s_m\right)\left(1-\gamma\right) - s_g\left(1 - s_m\right)\right]} \tag{55}$$

The next step is to set the desired characteristics of the compensation element in terms of stiffness (K_{comp}) and of force ($F_{comp}\Big|_{x=x_{\min}}$), delivered at position $x = x_{min} = S\,(1-\gamma)\,/\gamma$.

Target behaviour	Value of k_{comp}
Balanced force variation in ON and OFF modes	$-\left(K_{MB}+K_A\right)/2$
Constant force in OFF mode	$-K_A$
Constant force in ON mode	$-K_{MB}$

Table 2. Suggested values for the compensation stiffness to achieve specific behaviour of the actuator

From (1) and (55) the stiffness K_A of the SMA element in the austenitic state is obtained.

Though the compensation stiffness (always negative) could be set as desired in the range $-K_{MB} \div -K_A$, Table 1 shows how to choose the value of K_{comp} to obtain favourable operating characteristics: for $K_{comp} = -K_A$, the force of the activated actuator is constant and for $K_{comp} = -K_{MB}$ the force of the deactivated actuator is constant. By setting $K_{comp} = -0.5(K_A + K_{MB})$, the deviation from uniformity of both states of actuator is minimized.

The compensator force the at position $x = x_{min}$ to obtain the desired behavior must be:

$$F_{comp}\Big|_{x=x_{\min}} = F_{ON} - K_A S\left(\frac{1-\gamma}{\gamma}\right) \tag{56}$$

The compensator always acts with a force increasing with x and opposite to the force delivered by the SMA element.

3.3.1. Case study: single SMA compensated actuator

In this section, the design procedure of a single SMA compensated actuator is carried out numerically for a generic system with the following technical specifications:

- Required stroke: 10mm
- Minimum force in the right to left displacement F_{ON}: 10N
- Minimum force in the left to right displacement F_{OFF}: -5N
- Minimization of the variation force in overall travel

The material considered is a Nitinol wire, with austenitic Young modulus E_a=75GPa, martensitic Young modulus E_{MA}=28GPa, bilinear gradient E_{MB}=5GPa, strain at the threshold of pseudo-plastic regime ε_g=0.4% maximum deformation ε_{adm}=4%.

The non dimensional groups are calculated as follows:

$$s_1 = \frac{E_A}{E_{MA}} = \frac{75}{28} = 2.68 \tag{57}$$

$$s_m = \frac{E_{MB}}{E_{MA}} = \frac{5}{28} = 0.18 \tag{58}$$

$$s_g = \frac{\varepsilon_g}{\varepsilon_{adm}} = \frac{0.004}{0.04} = 0.1 \tag{59}$$

An optimal value for the ratio γ=0.75 can be chosen as a tradeoff between axial dimension and oversizing of the active SMA elements.

From (55) it is possible to obtain the cold state stiffness of the SMA wire:

$$K_{MA} = \frac{\gamma\left(F_{ON} - F_{OFF}\right)}{S\left[\left(s_1 - s_m\right)\left(1-\gamma\right) - s_g\left(1 - s_m\right)\right]} = \frac{0.75\left[10 - \left(-5\right)\right]}{10\left[\left(2.68 - 0.18\right)\left(1 - 0.75\right) - 0.1\left(1 - 0.18\right)\right]} = \\ = 2.07\frac{N}{mm} \tag{60}$$

Considering (1) and (51) and the last expression the cold state stiffness K_A and the post elastic martensitic stiffness K_{MB} can be obtained:

$$K_A = s_1 K_{MA} = 2.68 \cdot 2.07 = 5.55 N/mm \tag{61}$$

$$K_{MB} = s_m K_{MA} = 0.18 \cdot 2.07 = 0.373 N/mm$$

From (53) is computed x_{adm} , the maximum elongation of the SMA wire:

$$x_{adm} = \frac{S}{\gamma} = \frac{10}{0.75} = 13.33 mm \tag{62}$$

Taking into account the maximum deformation of the material ε_{adm} the wire length l_0 is:

$$l_0 = \frac{x_{adm}}{\varepsilon_{adm}} = \frac{13.33}{0.04} = 333.3 mm \tag{63}$$

From the austenitic stiffness and the wire length the wire diameter d is immediately obtained:

$$d = \sqrt{\frac{4K_A l_0}{E_A \pi}} = \sqrt{\frac{4 \cdot 5.55 \cdot 333.3}{75000\pi}} = 0.177 mm \tag{64}$$

The compensator system preload is obtained through (56).This value is negative because in its minimum stroke position $x = x_{min}$= 3.33mm, the preload is opposed to SMA active element action:

$$F_{comp}\Big|_{x=x_{\min}} = F_{ON} - K_A S\left(\frac{1-\gamma}{\gamma}\right) = 10 - 5.55 \cdot 10\left(\frac{1-0.75}{0.75}\right) = -8.5 N \tag{65}$$

In order to minimize the force fluctuations in both travel directions the optimum stiffness of compensation system is obtained from (Table 1) and is:

$$k_{comp} = -\frac{K_{MB} + K_A}{2} = -\frac{0.373 + 5.55}{2} = -2.96\frac{N}{mm} \tag{66}$$

3.4. Design of compensated actuators with two antagonistic SMA elements

The input data required for the design of a two antagonistic shape memory actuators are: the value of the minimum useful forces in the two directions of activation F_{ON1}, F_{ON2} the value of the stroke desired, S, and the active elements material characteristics (i.e. s_1, s_m and s_g). In the following equations, assuming that the axis of the actuator is horizontal, the forces are assumed positive when directed from right to left and negative when directed from left to right. The displacements are assumed positive from left to right.

For a compensated actuator with two antagonistic SMA element it can be shown [21] that it is always possible to set the ratio γ (53) to 1, so that the actuator stroke is equal to the maximum deflection imposed on the SMA elements (x_{min}=0).

If both active elements are constituted by the same alloy (same parameters s_1, s_m, s_g) is possible to demonstrate [21] that the optimum rigidity of the two elements will be equal (K_{A1}=K_{A2}=K_A and K_{MB1}=K_{MB2}=K_{MB}).

The force generated by element 1 in the ON state is:

$$F_{SMA1_ON} = K_A x \tag{67}$$

In the OFF state, using (3) for the martensite behavior, the force in element 1 is:

$$F_{SMA1_OFF} = F_{0m} + K_{MB} x \tag{68}$$

For element 2, the force output depends on the difference between the prestretch p of the two SMA elements and the position of the actuator. Assuming γ=1 the prestretch p is equal to the stroke S, and the force of element 2 in the ON and OFF state is respectively:

$$F_{SMA2_ON} = -K_A(S - x) \tag{69}$$

$$F_{SMA2_OFF} = -F_{0m} - K_{MB}(S - x) \tag{70}$$

The force delivered from the compensator is:

$$F_{comp} = F_{0comp} + k_{comp} x \tag{71}$$

where F_{0comp} indicates the force of the compensator at position $x = 0$.

Figure 9 shows the force displacement diagram of a two-SMA actuator and helps to understand the relationship between the variables involved in the equations.

Line OA in Figure 9 represents the characteristics of the austenitic (hot) SMA1 element. Segment BC represents the martensitic (cold) response of the antagonistic SMA2 element. Line DE is the characteristic of the compensation spring, with point D corresponding to the centerpoint of the total stroke S of the actuator. Line EG represents an ideally constant external load of amplitude F_{ON1}. The situation beyond point D is obtained by extrapolating linearly all the characteristic lines shown in Figure 9. Line AE corresponds to the characteristic of the SMA1 element and the compensation spring combined. At any position x, the difference between lines AE and BC gives the net output force of the actuator ($F_{net\ ON1}$) when element SMA1 is activated. When element SMA1 is disabled and SMA2 is enabled, the chart becomes similar to Figure 9, with all the lines mirrored with respect to the line AD.

The optimal performance of the actuator in Figure 9 is achieved when lines AE is parallel to line BC, so that the net output force of the actuator ($F_{net\ ON1}$) equals the external load (F_{ON1}) at any position x. Scirè and Dragoni [21] demonstrated that the optimal actuator meets the design specifications (i.e. the given output forces F_{ON1}, F_{ON2} and the net stroke S) when the following relationships hold true:

$$K_{MA} = \frac{\left(F_{ON1} - F_{ON2}\right)}{S\left[\left(s_1 - s_m\right) + 2s_g\left(s_m - 1\right)\right]} \tag{72}$$

$$k_{comp} = -\frac{\left(F_{ON1} - F_{ON2}\right)\left(s_1 + s_m\right)}{S\left[\left(s_1 - s_m\right) + 2s_g\left(s_m - 1\right)\right]} \tag{73}$$

$$F_{0comp} = \frac{s_g\left(F_{ON1} + F_{ON2}\right)\left(s_m - 1\right) + \left(F_{ON1}s_1 - F_{ON2}s_m\right)}{\left(s_1 - s_m\right) + 2s_g\left(s_m - 1\right)} \tag{74}$$

The force generated by the actuator in the case of element 1 ON and element 2 OFF is:

$$F_{net_ON1} = K_A x + F_{0comp} + k_{comp}x - F_{0m} - K_{MB}\left(S - x\right) \tag{75}$$

while the force generated in the case of element 2 ON and element 1 OFF is:

$$F_{net_ON2} = F_{0m} + K_{MB}x + F_{0comp} + k_{comp}x - K_A\left(S - x\right) \tag{76}$$

From (1) and (55) the stiffness K_A of the SMA element in the austenitic state is obtained.

The actuator designed by (72)-(74) provides a constant force in both directions. In the compensated actuators with two SMAs, the force of the compensator becomes zero and changes sign at mid-stroke. In the range $0 < x < S/2$ the force of the compensator has the same direction as the force exerted by element 1, while in the range $S/2 < x < S$ it has the same direction as the force generated by element 2.

3.4.1. Case study: Double SMA compensated actuator

This section describes the design of double SMA compensated actuator under the hypothesis of using traction Nitinol springs with the following characteristics:

- Wire diameter: 0.65mm
- Mean coil diameter: 6.8mm
- Number of active coils: 25.5
- Free length: 25mm
- Austenitic stiffness: K_A: 0.0615N/mm
- Martensitic stiffness: K_{MA}: 0.0414N/mm
- Pseudo-plastic stiffness: K_{MB}: 0.0156N/mm
- Deflection at the threshold of pseudo-plastic regime x_g: 23mm

The desired output stroke is S =75mm, with the maximum possible force in both directions.

In this case the dimensional parameter γ can be taken equal to one and consequently the maximum extension of the active elements x_{adm} is equal to the desired stroke S.

The non dimensional parameters are:

$$s_1 = \frac{K_A}{K_{MA}} = \frac{0.0615}{0.0414} = 1.486 \tag{77}$$

$$s_m = \frac{K_{MB}}{K_{MA}} = \frac{0.0156}{0.0414} = 0.377 \tag{78}$$

$$s_g = \frac{x_g}{x_{adm}} = \frac{23}{75} = 0.306 \tag{79}$$

Using the above dimensionless parameters, eq. (72) gives the maximum force differential $(F_{ON1} - F_{ON2})$ that the actuator can produce in both directions as:

$$\begin{aligned} &F_{ON1} - F_{ON2} = K_{MA} S\left[\left(s_1 - s_m\right) + 2s_g\left(s_m - 1\right)\right] = \\ &= 0.0414 \cdot 75\left[\left(1.486 - 0.377\right) + 2 \cdot 0.306\left(0.377 - 1\right)\right] = 2.26N \end{aligned} \tag{80}$$

Assuming that the actuator generates the same output force regardless of the direction of motion gives:

$$F_{ON1} = -F_{ON2} = 1.13N \tag{81}$$

From (73) the overall stiffness of the compensation system k_{comp} is calculated:

$$\begin{aligned} k_{comp} &= -\frac{\left(F_{ON1} - F_{ON2}\right)\left(s_1 + s_m\right)}{S\left[\left(s_1 - s_m\right) + 2s_g\left(s_m - 1\right)\right]} = -\frac{2.26\left(1.486 + 0.377\right)}{75\left[\left(1.486 - 0.377\right) + 2 \cdot 0.306\left(0.377 - 1\right)\right]} = \\ &= -0.0771N / mm \end{aligned} \tag{82}$$

Likewise, (74) gives the force F_{0comp} that the compensator must apply to the SMA elements at the position $x = 0$:

$$F_{0comp} = \frac{s_g\left(F_{ON1}+F_{ON2}\right)\left(s_m-1\right)+\left(F_{ON1}s_1-F_{ON2}s_m\right)}{\left(s_1-s_m\right)+2s_g\left(s_m-1\right)} = \\ = \frac{0.306\left[1.13+\left(-1.13\right)\right]\left(0.377-1\right)+\left[1.13\cdot 1.486-\left(-1.13\right)\cdot 0.377\right]}{\left(1.486-0.377\right)+2\cdot 0.306\left(0.377-1\right)} = 2.893N \tag{83}$$

3.5. Design of the compensator system

This section describes the elastic constants of the shape memory elements and the maximum deflections that they will undergo, calculated from the design data (force and stroke required of the actuator) following the procedure of the previous section. Thanks to these parameters the shape memory elements (wires or springs) can be described using classical engineering formulas. The method also provides the properties needed by the elastic compensation to meet the required performance. Two elastic compensation systems are described in detail in this section: 1) a rocker-arm mechanism and 2) a double articulated quadrilateral.

3.5.1. Rocker-arm compensator

The compensation mechanism shown in Figure 10 is made up of a rocker-arm R hinged in G to the frame T. The (conventional) compensation spring S_c (with free length L_{0Trad} and spring rate k_{Trad}) connects the extremity F of the shortest side of the rocker-arm to point E of the frame. Point O (the output port of the actuator) is used to connect the primary elastic elements of the actuator (SMA1 and SMA2), which are also fixed at points P and Q to the frame. In the case of a single-SMA actuator, the active element (SMA1) is placed at the bottom of the device, element SMA 2 disappears and the contrasting element is made up by the conventional compensation spring, S_c.

The mechanism in Figure 10 has a position of unstable equilibrium, corresponding to the configuration where the axis EF of the compensation spring S_c passes through the hinge G of the rocker-arm. In this position, the force exerted by the compensator on the slider O is null. In the case of an actuator with a single active element, the compensation spring S_c is always placed to the right of hinge G in order to exert a contrasting force on the SMA element 1 needed to deform it in the cold state. For an actuator with two opposing SMA elements, the spring S_c is located in an unstable position (line EF passes through G) when point O is at the center of the stroke (S). In this way, the compensation mechanism helps active element SMA1 for the lower half of the stroke and the element SMA2 for the upper half of the stroke. If in Figure 10 the absolute value of the angle γ is small, i.e. if $l_0+x-(a+d) << c$ then the following expressions apply with good approximation:

$$F_{comp}(x) = -\frac{abF_{Trad}\beta}{c\left(a+b\right)} \tag{84}$$

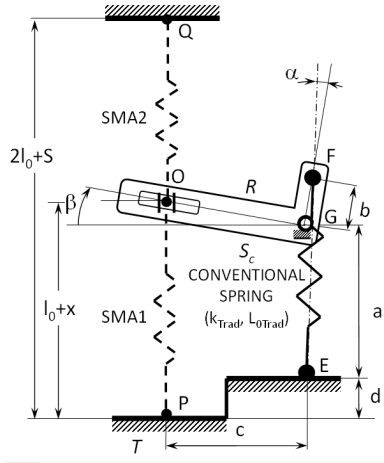

Figure 10. Oscillating rocker arm compensation mechanism

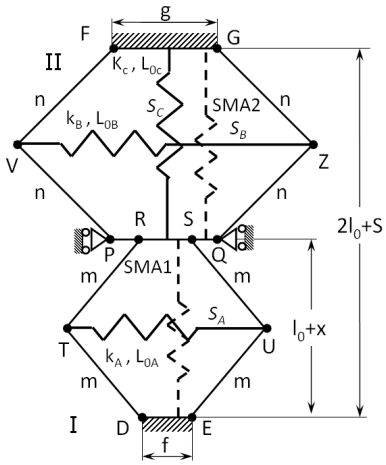

Figure 11. Double articulated quadrilateral compensation mechanism

$$k_{Comp} = \frac{\partial F_{Comp}}{\partial x} = -\frac{abF_{Trad}}{(a+b)c^2} \tag{85}$$

When lengths *b,c,d* have been arbitrarily decided along with the stiffness of the traditional spring k_{Trad}, from (84) (calculated for $x=x_{min}$) and (85) the expressions for a and L_{0Trad} are derived which define the correct sizing of the compensation mechanism:

$$L_{0Trad} = \frac{\left[k_{comp}\left(A-b+d-l_0\right)+F_{comp}\Big|_{x_{\min}}\right]\left(c^2\,k_{comp}^2\,\gamma - B\right)}{B\,k_{comp}} \tag{86}$$

$$a = l_0 - A - d - \frac{F_{comp}\Big|_{x_{\min}}}{k_{comp}} \tag{87}$$

with:

$$A = S\left(\frac{\gamma - 1}{\gamma}\right) \tag{88}$$

$$B = b\,k_{Trad}\,\gamma\left[k_{comp}(d - l_0 + A) + F_{comp}\Big|_{x_{\min}}\right] \tag{89}$$

In Equations (86) – (89) the term $F_{comp}\Big|_{x_{\min}}$ is given by (56) or by (74) respectively for the single SMA or two opposing SMAs actuator. Likewise, the stiffness k_{comp}, is obtained from Table 1 or from (73) for single SMA or for the two opposing SMAs actuator respectively.

3.5.2. Double articulated quadrilateral compensator

Figure 11 illustrates a second elastic compensation system based on the use of two articulated quadrilaterals (I and II), which are connected together in series. The first quadrilateral (I) is made up of four equal rods DT, EU, RT and SU, hinged together in T and U and fixed to the frame with hinges D and E. In the upper part, the rods are hinged in R and S to the bar PQ, which can translate vertically. The rods DT, EU, RT and SU have length *m*, while the horizontal segments DE and RS have length *f*. The conventional spring S_A, with stiffness k_A and free length L_{0A}, is stretched between hinges T and U.

The second quadrilateral (II) is made up of four equal rods VP, ZQ, VF and ZG, connected with internal hinges in V and Z and fixed to the frame with hinges F and G. The length of the rods VP, ZQ, VF and ZG is *n*, while the length of the horizontal segments PQ and FG is *g*.

Quadrilateral II contains two conventional springs, S_B and S_C. Spring S_B, with stiffness k_B and free length L_{0B}, is stretched horizontally between hinges V and Z. Spring S_C, with stiffness k_C and free length L_{0C}, is stretched vertically between the horizontal sides FG and PQ. Member PRSQ, which is common to the two quadrilaterals, represents the output ports of the actuator. In addition to the conventional springs, S_A, S_B and S_C, the mechanism in Figure 11 contains also the primary active elements of the actuator. Active element SMA1 is hosted by the quadrilateral I and connects the base DE to the output port PRSQ. The second primary element SMA2 (if applicable) is hosted by quadrilateral II and connects the frame FG to the output port PRSQ.

For the sake of simplicity, all the springs shown in Figure 11 (both SMA and conventional) are traction springs. However, the mechanism can work just as well with all compression springs, which can be designed with the same equations presented below.

By imposing the vertical equilibrium of the member PRSQ in Figure 11 and excluding the forces exerted by the shape memory elements, it is possible to obtain the compensation force as a function of the position *x* of the output port.

Imposing that:

$$L_{0A} = f \qquad L_{0B} = g \qquad k_B = k_C \tag{90}$$

the compensation force becomes:

$$F_{comp}(x) = -k_A(l_0 + x) + k_C L_{0C} \tag{91}$$

i.e. it depends linearly on x as desired in an ideal compensation system. The compensation stiffness implied in (91) is:

$$k_{comp} = \frac{\partial F_{comp}}{\partial x} = -k_A \tag{92}$$

From (91) the force exerted by the compensation system at $x=x_{min}$ is:

$$F_{comp}\Big|_{x=x_{min}} = -k_A(l_0 + x_{min}) + k_C L_{0C} \tag{93}$$

Conditions (92) and (93) complete the design of the compensation mechanism in Figure 11. The value k_{comp} is taken from Table 1, for the case of a single SMA, or alternatively from (73) for two SMA elements. Similarly, the value $F_{comp}\Big|_{x=x_{min}}$ is taken from (56) or (74), for one or two SMA elements, respectively.

By solving (93) with respect to the product $k_C L_{0C}$, you can get the correct design of spring S_C. From condition (90), we see that the springs S_B and S_C must have the same stiffness and that the free length of spring S_B must be g. It is thus convenient to set to g the free length of spring C as well, so as to have two identical springs S_B and S_C in quadrilateral II with spring rate:

$$k_C = k_B = \left(F_{comp}\Big|_{x=x_{min}} + k_A(l_0 + x_{\min}) \right) \Big/ g \tag{94}$$

4. General discussion

4.1. Performances of the uncompensated SMA actuators

The analytical framework described in Paragraph 3 considers both dissipative and conservative forces acting on the system. Closed-form relationships are developed, which are the basis of a step-by-step procedure for an optimal design of the entire actuator (both with antagonist SMA, bias elastic element or backup force). Specific formulas for dimensioning of the SMA element in the form of straight wires and helical traction springs are also presented.

The physical meaning of dimensionless design parameters s_1, s_2, s_F and s_0 deserves specific comments. Parameter s_1 is an intrinsic property of the SMA material, the higher s_1, the better the SMA behaviour. Parameter s_2 is a measure of the relative stiffness between the bias spring (be it traditional or SMA) and the primary SMA spring. Optimal values of parameter

s_2 maximize the overall travel. Low values of s_2 lead to an increase in stroke and in the actuator dimension. Parameter s_F quantifies the influence of dissipative forces on the stroke of the actuator. For low values of s_F the dissipative force is negligible in comparison with the forces expressed by the backup systems and the actuator moves freely. The upper limit of s_F is reached when the dissipative force becomes high enough to prevent the movement of the actuator. Parameter s_0, is the equivalent of s_F for the conservative force. Since the conservative force helps the backup system, high values of s_0 improve the actuator performances.

Also for the three backup systems analyzed, some specific comments are reported. Using a force as back up for the primary spring may be convenient when there is important conservative force acting on the system which helps the restoring process. Often this solution is not feasible due to dimensional constraint which prevents dead loads to be used. The binary actuator with a traditional spring backup gives the worst performances in terms of output characteristic, due to disadvantages of the elastic slope of the traditional spring. By analyzing Section 3.2 equations it is found that for a given cursor stroke, Δx the optimal value of s_2 provided by (21) minimizes the pre-stretch of the system, p, and tends to minimize the total size of the actuator. Eq.(18) shows that the pre-stretch of the system, p, acts on the stroke, Δx, as a pure gain. Figure 12a displays the normalized stroke, $\Delta x/p$, as a function of the other variables: s_0 (used as parameter of the family of surfaces), s_2 and s_F (these two variables are plotted along the axes), taking $s_1=3$ because this is a typical value for the elastic moduli ratio of commercial shape memory alloy. Eq. (18) and Figure 12a also highlight that for each combination of s_0 and s_F exists an optimal value, s_2^*, of parameter s_2 which maximizes the normalized stroke. Eq. (19) shows that for each combination of s_1 and s_F the stroke increases monotonically when parameter s_2 decreases, implying a more flexible bias spring. Both equations (18) and (19) prove that meaningful strokes ($\Delta x>0$) are only possible if parameter s_F is lower than s_{Fcr} of equation (10).

Section 3.3 shows that the binary actuator with a SMA spring backup gives the best performances in terms of output characteristic, both respect to elastic backup and bias force backup. Equation (30) shows that also in this case the pre-stretch of the system, p, acts on the stroke, Δx, as a pure gain. Figure 12b displays the normalized stroke, $\Delta x/p$, as a function of the other variables: s_0 (used as a parameter of the family of surfaces), s_2 and s_F (these two variables are plotted along the axes), taking $s_1=3$ (a typical value for elastic moduli in austenitic and martensitic phase of a commercial SMA). Equation (30) and Figure 12b also highlight that for each combination of s_1 and s_F an optimal value, s_2^*, of parameter s_2 exists that maximizes the normalized stroke. Equation (30) shows that for each combination of s_1 and s_F the stroke increases monotonically when parameter s_2 decreases, implying a more flexible SMA bias spring. Correspondingly, equation (29) shows that the pre-stretch of the system, p, tends to infinity. If (31) is used to choose s_2, the global pre-stretch, p, is minimized and the total length of the actuator tends to be reduced, but it is not minimized. To obtain a value of s_F and a value of s_2 able to minimize the total length of the actuator, expressions that depend on the embodiment of the springs are needed.

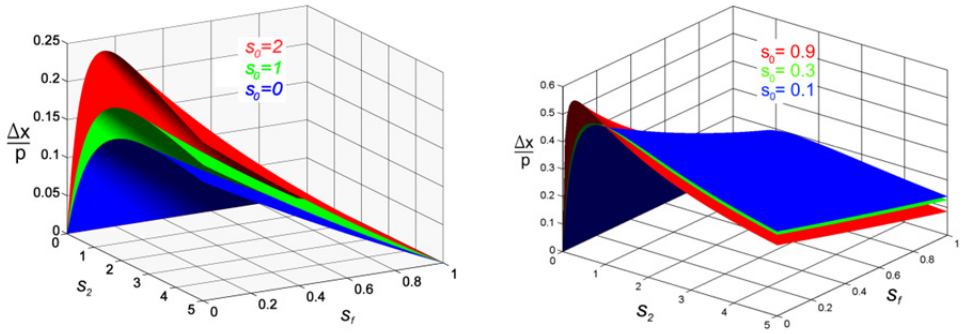

Figure 12. Normalized stroke of a shape memory actuator backed up by a traditional spring (a) or by an antagonist SMA spring (b) as a function of the parameters s_2 , s_F and s_0.

4.2. Performances of the compensated SMA actuators

The performances of SMA compensated actuators are improved compared to traditional SMA actuators. A comparison between a traditional and a compensated SMA actuators, being equal the active elements and their maximum deformations, shows that the compensated system has longer strokes. Conversely, being equal the output stroke, the deformations in the compensated SMA system are lower than the traditional one. In general the compensated SMA actuator is able to obtain the same performances of a traditional system with lower maximum deformation in the material, while for a given admissible deformation the active elements of a compensated SMA are more stressed because they work against both the external load and the compensation system during the first part of the stroke. The energy stored in the compensator is released in the second part of the stroke helping in keeping the output force constant.

Experimental comparative tests on a SMA actuator with or without a rocker-arm compensator [28] demonstrated that the stroke of the compensated system is always greater regardless the external load. The stroke incremented by 2.5 times with no load up to 22 times with the maximum design force applied. Furthermore, the net stroke of the compensated actuator is not dependent on the applied force. This peculiarity simplifies both the design and the selection of the actuator for a given application. Other remarkable advantages of the compensated actuator lie in the nearly-constant value of the output force and in the fastest response compared to traditional systems, even with longer output strokes. The fastest response is due to the lower difference between internal external forces in the end positions. By contrast, the response time (the time needed to achieve an incipient displacement) is considerably longer for the compensated actuator. This behaviour is due to the high stress at which the SMA springs operate before activation, which requires a greater

degree of martensite-austenite transformation (hence a greater temperature) to start the motion. In general, the compensated actuator has no intrinsic positions of stable equilibrium so mechanical hard stops are needed to prevent dangerous over deformation in the SMA. One hard stop provides a monostable behaviour for the single SMA, the two hard stops needed for the double SMA produces a bistable behaviour. The characteristic of mono or bistability leads to great operative advantages because the actuator is able to: maintain a specific position even without power; achieve precise and repetitive positioning; facilitate control strategies of the overall system.

5. Conclusion

The optimum mechanical design of shape memory based actuators is performed by means of analytical description of the governing equations of the system, providing an easy to follow design procedure for engineers working with SMA devices. Since no complex thermo-mechanical models are involved, the closed form equations developed are based on two simple constitutive models: a linear or a bilinear behaviour for the martensitic phase and a linear relationship for the austenitic phase. Three backup elements are considered to recover the stroke: a constant force, a traditional elastic spring and antagonist SMA element, leaving the designer the opportunity to adopt those which fits the application best. The external load is as general as possible, because a system of both dissipative and conservative forces is taken into account. The actuator performances are improved considering an elastic compensation instead of a backup element. This negative stiffness element can enhance either the stroke or the force of the SMA actuator depending on the needs. The output force design equations both for the SMA actuators and for the compensator are given and the detailed description of the compensated SMA system grants an immediate comprehension of the whole system. In order to give an operative guideline for SMA actuators design, several numerical examples are provided. The proposed procedure is applied to real case studies and to a specific configuration of SMA active elements (wires or springs). The benefits of the described methodology are critically discussed and compared. In terms of mechanical performance the agonist antagonist SMA system gives the best performances both for compensated and uncompensated systems, while optimum values for the non dimensional parameters are provided in order to obtain compact and efficient SMA based actuators. The analytical equations developed in this Chapter allow a SMA based actuator to be correctly designed in order to match the specifications and give useful information to optimize size and mechanical response of the system with no need of complex numerical simulations.

Author details

A. Spaggiari*, G. Scirè Mammano and E. Dragoni
Department of Science and Methods for Engineering, University of Modena and Reggio Emilia, via Amendola, Campus S. Lazzaro Reggio Emilia, Italy

* Corresponding Author

6. References

[1] Otsuka K Wayman C M (2002) Shape memory Materials, Cambridge University Press, Cambrdige UK.

[2] Lagoudas DC, (2008) Shape Memory Alloys Encyclopedia of Aerospace Engineering John Wiley & Sons, New York.

[3] Boyd JG, Lagoudas DC (1996) A Thermodynamical Constitutive Model for Shape Memory Materials. Part I. Int. J. Plast 12(6): 805-842.

[4] Arghavania J, Auricchio F, Naghdabadia R and Sohrabpoura S (2009) A 3-D phenomenological constitutive model for shape memory alloys under multiaxial loadings Int. J. Plast. 26(7): 976-991.

[5] Kuribayashi, K. (1989) Millimeter-sized Joint Actuator using a Shape Memory Alloy, Sensor Actuator, 20(1-2): 57-64.

[6] Mertmann M, Vergani G (2008) Design and application of shape memory actuators, Eur. Phys. J. Special Top. 158:221–230.

[7] Kim B, Lee MG, Lee YP, Kim YI, Lee GH (2006) An earthworm-like micro robot using shape memory alloy actuator, Sensors and Actuators A: 125(2): 429-437,

[8] Reynaerts D. Van Brussel H (1998) Design aspects of shape memory actuators Mechatronics, 8: 635-656.

[9] Lu A, Grant D, Hayward V (1997) Design and comparison of high strain shape memory alloy actuators" Proc.IEEE Robotics and Automation 1(20): 260-265.

[10] Bergamasco M, Dario P Salsedo F (1990) Shape Memory Alloy Microactuators Sensors Actuators A 21(1-3): 253-257.

[11] Nespoli A, Besseghini S, Pittaccio S, Villa E, Viscuso S (2010) The high potential of shape memory alloys in developing miniature mechanical devices: A review on shape memory alloy mini-actuators. Sensors and Actuators A: Physical 158(1): 149-160.

[12] Jansen S, Breidert J Welp EG (2004) Positioning actuator based on shape memory wires, ACTUATOR Proc. of 9th International Conference on New Actuators.

[13] Strittmatter J, Gümpel P (2004) Shape memory actuator for hydraulic valve ACTUATOR Proc. of 9th International Conference on New Actuators.

[14] Bellini A, Colli M, Dragoni E (2009) Mechatronic Design of a Shape Memory Alloy Actuator for Automotive Tumble Flaps: A Case Study, IEEE Trans on Industrial Electronics, 56(7):2644-2656.

[15] Haga Y et al. (2005) Dynamic Braille display using SMA coil actuator and magnetic latch, Sens. Actuators A, 119: 316-322.

[16] Elwaleed AK, et al., (2008) A new method for actuating parallel manipulators, Sens. Actuators A 147:593–599.

[17] Migliavacca F. et al. (2004) Stainless and shape memory alloy coronary stents: a computational study on the interaction with the vascular wall, Biomechan Model Mechanobiol 2:205-217.

[18] Spinella I, Dragoni E (2009) Design equations for binary shape memory actuators under dissipative forces. Pro Insn Mech Engrs C: J. Mech. Eng. Sci 223(C3): 531–543.

[19] Spinella I, Scirè Mammano G, Dragoni E (2009) Conceptual design and simulation of a compact shape memory actuator for rotary motion. J. Mater. Eng. Perform. 18(5-6): 638–648.

[20] Spaggiari A, Spinella I, Dragoni E (2012) Design equations for binary shape memory actuators under arbitrary external forces, Journal of Intelligent Material Systems and Structures (In press) DOI: 10.1177/1045389X12444491

[21] Scirè Mammano G, Dragoni E (2011) Increasing stroke and output force of linear shape memory actuators by elastic compensation. Mechatronics 21(3): 570-580.

[22] Spaggiari A, Spinella I, Dragoni E (2011) Design of a Telescopic Linear Actuator Based on Hollow Shape Memory Springs, J. Mater. Eng. Perform. 20: 489-496.

[23] Scirè Mammano G, Dragoni E (2011) Modelling of Wire-on-Drum Shape Memory Actuators for Linear and Rotary Motion". J. Intell. Mater. Syst. Struct. 22(11): 1129-40

[24] Lagoudas D C, Miller D A, Rong L, Kumar P K (2009) Thermomechanical fatigue of shape memory alloys. Smart Materials and Structures 18:085021.

[25] Scirè Mammano G, Dragoni E (2012) Functional fatigue of Ni–Ti shape memory wires under various loading conditions. Int. J. fatigue (In press) http://dx.doi.org/10.1016/j.ijfatigue.2012.03.004

[26] Budynas R, Nisbett R, (2006) Shigley's Mechanical Engineering Design, McGrow Hill, New York.

[27] Berselli G, Vertechy R, Vassura G, Parenti Castelli V (2009) Design of a single-acting constant-force actuator based on dielectric elastomers. J Mech Robot 1 (3): 031007.1:031007.7.

[28] Scirè Mammano G, Dragoni E (2011) Design and Testing of an Enhanced Shape Memory Actuator Elastically Compensated by a Bi-Stable Rocker-Arm. Proc.ASME SMASIS Conference 18 – 21, Scottsdale, Arizona, USA, ISBN: 978-0-7918-4415-1.